Electronic Supplementary Information

Substituent engineering of the diboron molecular architecture for a nondoped and ultrathin emitting layer

Tien-Lin Wu,*[a] Jian Lei,[ab] Chia-Min Hsieh,[a] Yi-Kuan Chen,[a] Pei-Yun Huang,[a] Po-Ting Lai,[c] Tsu-Yu Chou,[c] Wei-Chen Lin,[d] Wei Chen,[d] Chi-Hua Yu[d], Liang-Yan Hsu,[b] Hao-Wu Lin[c] and Chien-Hong Cheng*[ae]

[a] Department of Chemistry, National Tsing Hua University, Hsinchu, 300044, Taiwan
[b] Institute of Atomic and Molecular Sciences, Academia Sinica, Taipei 10617, Taiwan
[c] Department of Materials Science and Engineering, National Tsing Hua University, Hsinchu, 300044, Taiwan
[d] Department of Engineering Science, National Cheng Kung University, Tainan, 701, Taiwan
[e] Department of Chemistry, National Sun Yat-sen University, Kaohsiung, 80424, Taiwan

E-mail: tlwu@mx.nthu.edu.tw
E-mail: chcheng@mx.nthu.edu.tw

Table of Contents:

Electronic Supplementary Information (ESI)

(A) General information

Chemical and characterization. All the experimental operations were performed under nitrogen; the equipment was dried in an oven at 110 °C for several hours. Starting material chemicals and reagents were purchased from commercial providers without further purification. Diethyl ether and toluene were distilled over sodium particles. NMR spectra using $CHCl_3/CDCl_3$ (δ 7.24/77.0 ppm) were recorded with a Varian Mercury 400 spectrometer. High-resolution mass (HRMS) was performed on JMS-T200GC AccuTOF GCx in field desorption (FD) source mode in the Instrumentation Center at NCTU. The single crystal suitable for X-ray diffraction was grown by sublimation. The X-ray diffraction was carried out on a Bruker X8 APEX X-ray diffractometer with Mo *K*α radiation (l = 0.71073 Å) and the structure was solved by SHELX 97 program in the Instrumentation Center at NTHU. Elemental analyses were performed using an analyzer (vario EL cube, Elementar) in Instrumentation Center at NCHU.

(B) Synthesis and characterization of iCzDBA

Scheme S1 Synthesis of 9-(4-bromo-3,5-diisopropylphenyl)-9H-carbazole and iCzDBA.

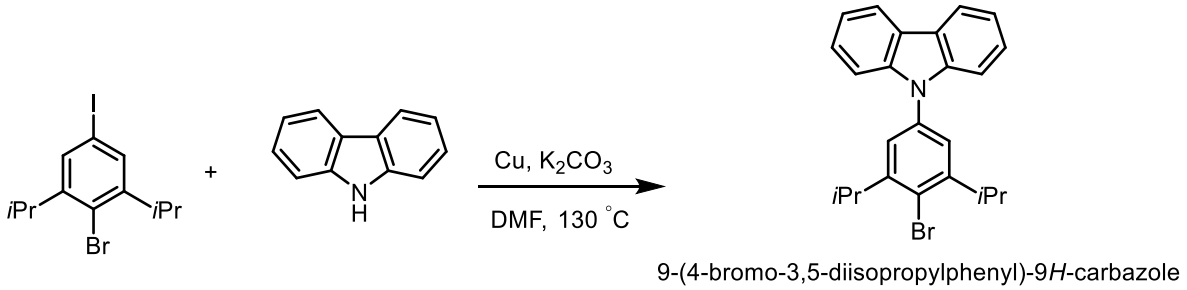

9-(4-bromo-3,5-diisopropylphenyl)-9*H*-carbazole

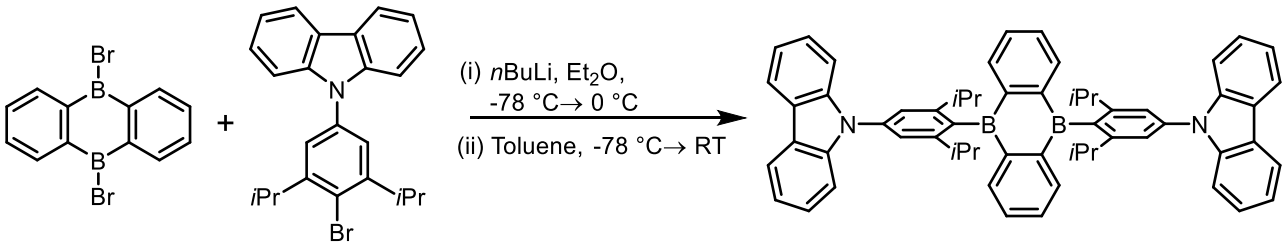

iCzDBA

Synthesis of 9-(4-bromo-3,5-diisopropylphenyl)-9*H*-carbazole. Under N_2 atmosphere, a stirred suspension of 2-bromo-5-iodo-1,3-diisopropylbenzene (2.00 g, 5.45 mmol), carbazole (1.00 g, 5.96 mmol), copper powder (1.06 g, 16.67 mmol), potassium carbonate (2.30 g, 16.67 mmol) and anhydrous N,N-dimethylmethanamide (16 mL) was heated at 130 °C for 24 h. The resulting mixture was filtered through Celite and extracted by dichloromethane/water. Organic phase was dried ($MgSO_4$) and removed in vacuo, and purified by column chromatography (silica gel, eluent: hexane/dichloromethane

= 10:1) to give the product as a white solid (1.95 g, 88%). ^{1}H NMR (400 MHz, $CDCl_3$): δ 8.14 (d, J = 8.0 Hz, 2H), 7.43-7.36 (m, 4 H), 7.32 (s, 2 H) 7.30-7.26 (m, 2 H), 3.61 (sep, J = 6.8 Hz, 2 H), 1.28 (d, J = 6.8 Hz, 12 H). ^{13}C NMR (100 MHz, $CDCl_3$): δ149.7, 140.6, 137.0, 126.0, 124.6, 123.4, 122.7, 120.4, 119.9, 109.7, 33.8, 23.0. FD-HRMS Calcd for $C_{24}H_{24}BrN$: 405.1087. Found: 405.1081.

Synthetic procedure of iCzDBA. Under N_2 atmosphere, *n*BuLi (2.5 M in hexane, 3.6 mL, 9.0 mmol) was added dropwise to a stirred solution of 9-(4-bromo-3,5-diisopropylphenyl)-9*H*-carbazole (2.4 g, 6.0 mmol) in an anhydrous Et_2O (170 mL) at -78 °C, and then the reaction mixture was warmed to 0 °C within 30 min. A solution of 9,10-dibromo-9,10-diboraanthracene (1.0 g, 3.0 mmol) in dry toluene (75 mL) was then added dropwise to reaction mixture at -78 °C. the reaction mixture was stirred overnight at room temperature. The mixture was extracted by $NH_4Cl_{(aq)}$ (60 mL) and dichloromethane (60 mL). All volatiles were removed in vacuo and the residue was further purified by column chromatography (silica gel, eluent: hexane/dichloromethane = 2:1) to obtain iCzDBA as a yellow solid (2.00 g, 81%). The compound was further purified by the temperature-gradient vacuum sublimation (under 10^{-6} torr), and the sublimed compound was used for chemical characterization, photophysical measurement, and device fabrication. ^{1}H NMR (400 MHz, $CDCl_3$): δ 8.19 (d, J = 7.6 Hz, 4 H), 7.81 (dd, J = 3.2, 5.4 Hz, 4 H), 7.63-7.59 (m, 8 H), 7.48 (td, J = 1.1, 7.1 Hz, 4 H), 7.43 (s, 4 H), 7.31 (td, J = 0.8, 7.0 Hz, 4 H), 2.57 (sep, J = 6.8 Hz, 4 H), 1.14 (d, J = 6.8 Hz, 24 H). ^{13}C NMR (100 MHz, $CDCl_3$): δ 151.3, 140.8, 139.0, 133.3, 125.8, 123.4, 120.3, 119.7, 110.1, 35.7, 24.1. FD-HRMS Calcd for $C_{52}H_{40}B_2N_2$: 826.4643. Found: 826.4644. Anal. Calcd for $C_{52}H_{40}B_2N_2$: C, 87.17; H, 6.83; N, 3.39. Found: C, 87.58; H, 6.64; N, 3.51.

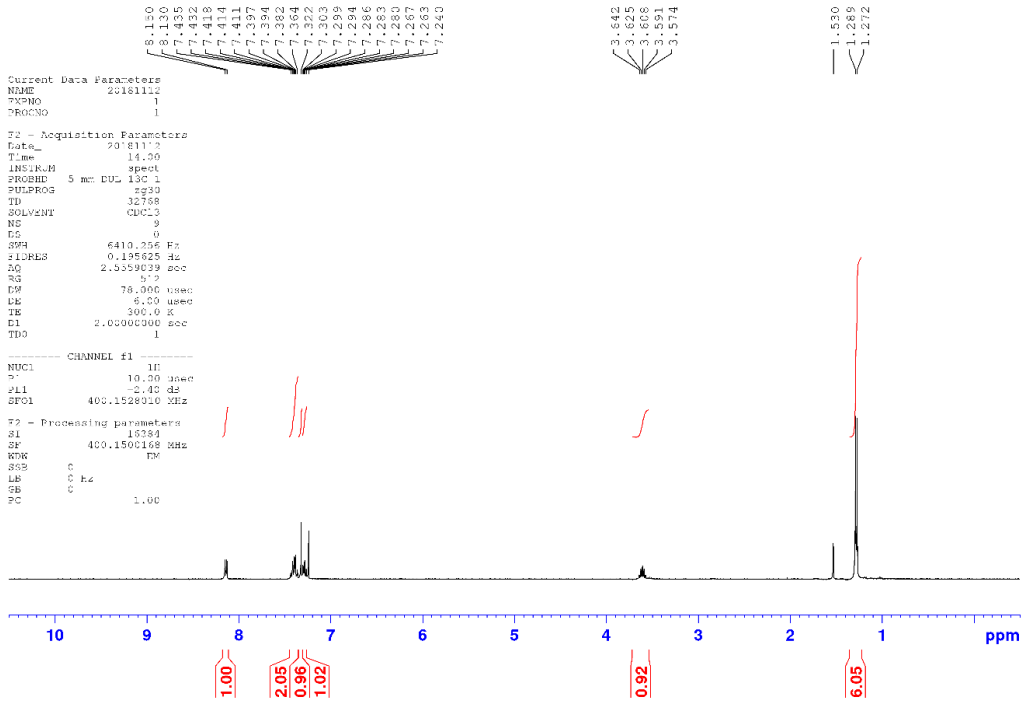

Fig. S1 ^{1}H NMR spectrum of 9-(4-bromo-3,5-diisopropylphenyl)-9*H*-carbazole.

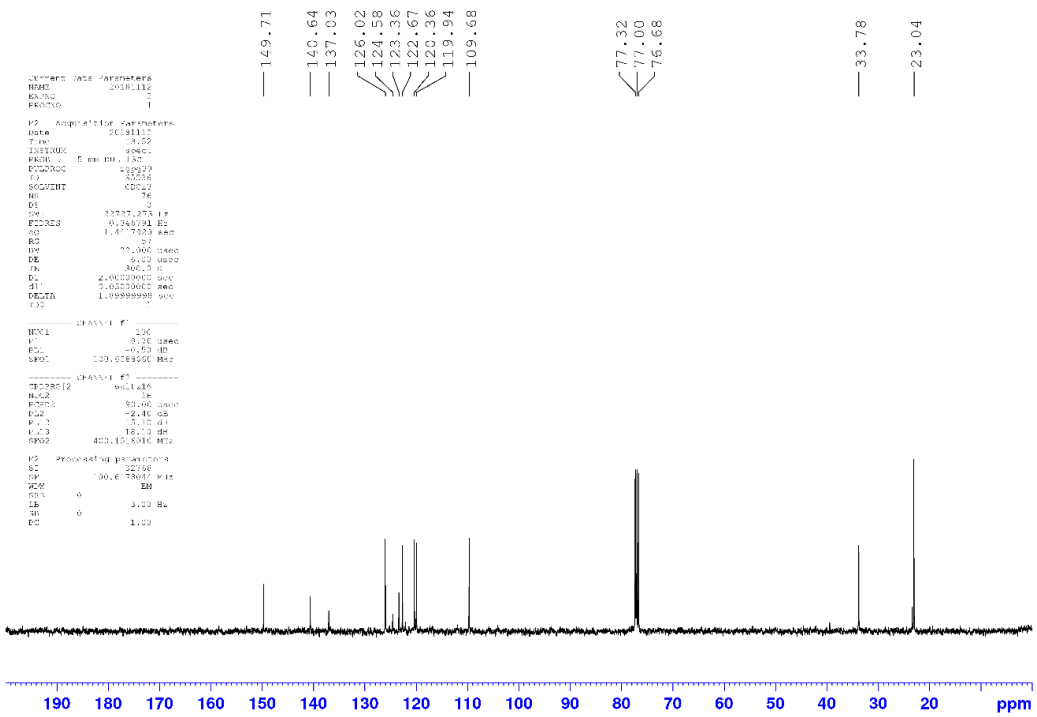

Fig. S2 ^{13}C NMR spectrum of 9-(4-bromo-3,5-diisopropylphenyl)-9*H*-carbazole.

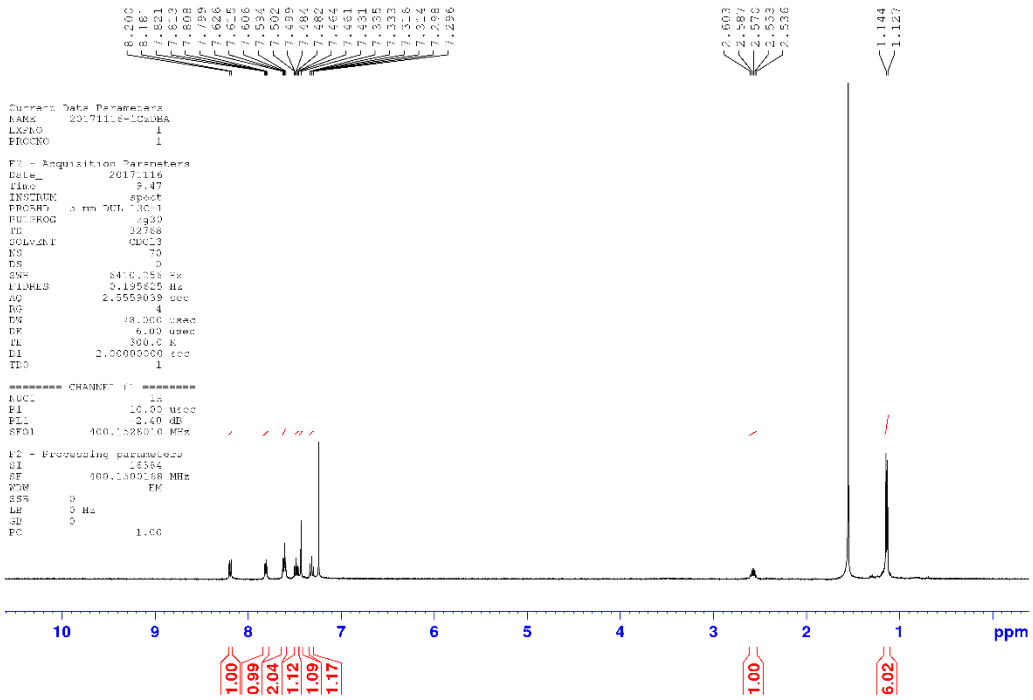

Fig. S3 ^{1}H NMR spectrum of iCzDBA.

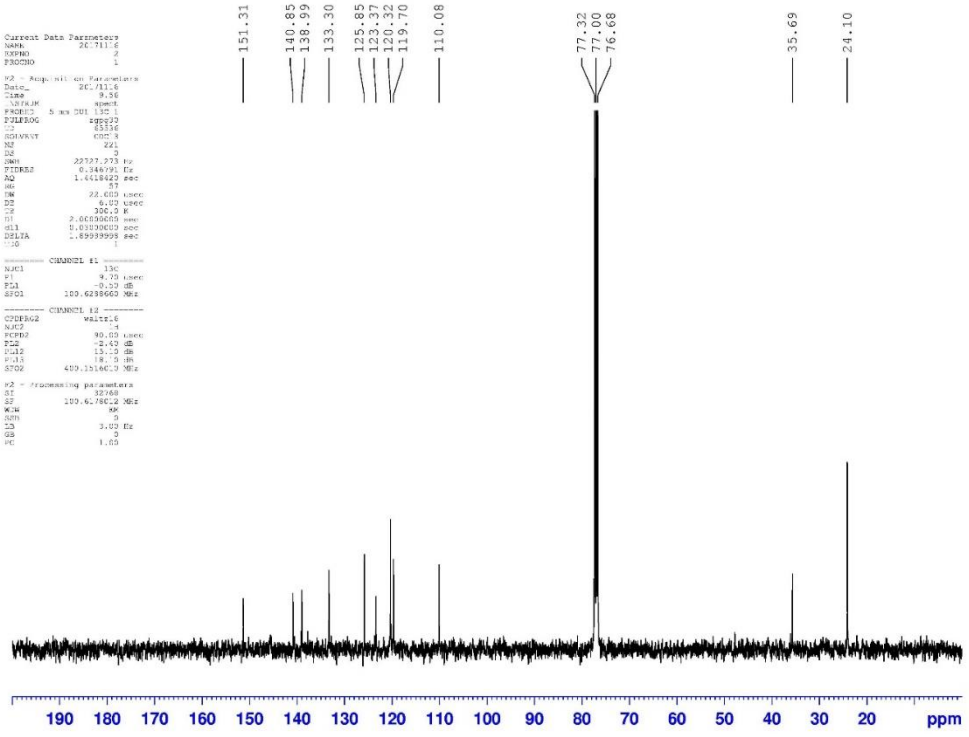

Fig. S4 ^{13}C NMR spectrum of iCzDBA.

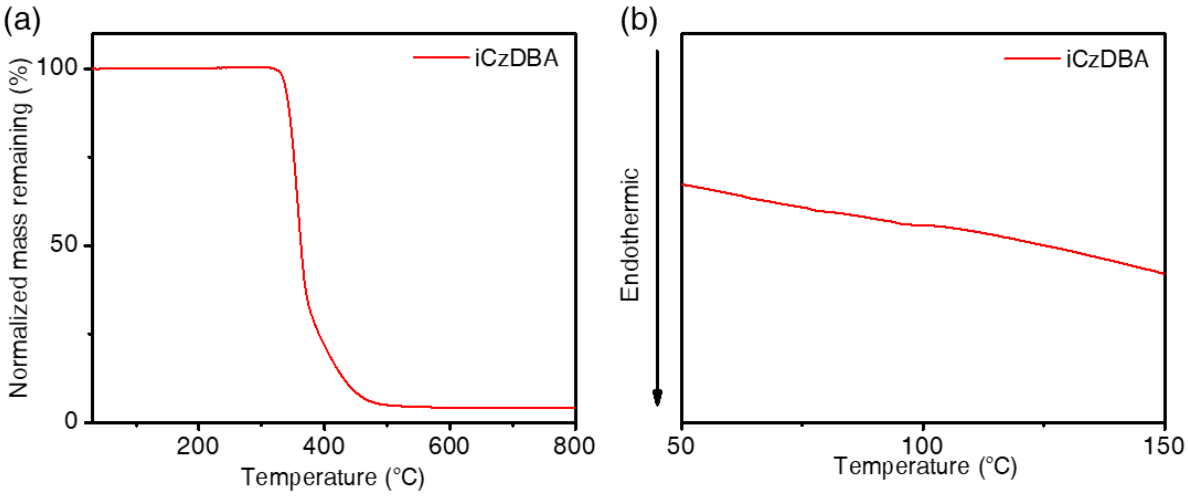

Fig. S5 (a) The thermal gravimetric analysis of iCzDBA. (b) The differential scanning calorimetry of iCzDBA.

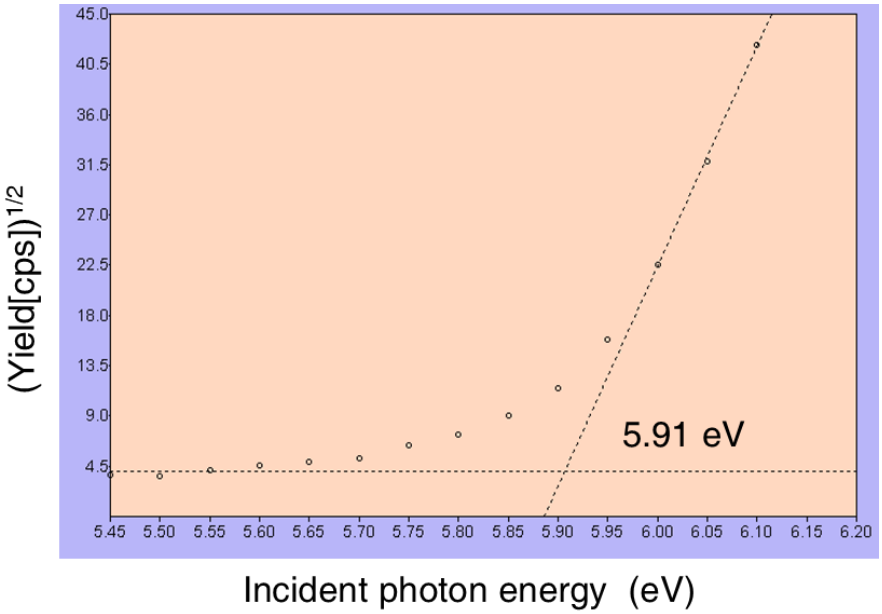

Fig. S6 The photoelectron spectrum of iCzDBA neat film.

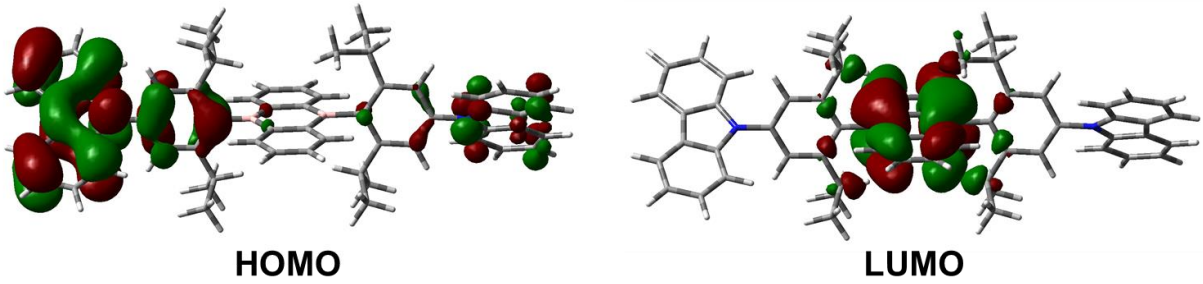

Fig. S7 Calculated HOMO/LUMO distributions of iCzDBA.

(C) X-ray diffraction and single-crystal analysis

Table S1 The crystal data and structure refinements of CzDBA, iCzDBA and *t*BuCzDBA.

Material	CzDBA	iCzDBA	*t*BuCzDBA
Empirical formula	$C_{52}H_{40}B_2N_2$	$C_{60}H_{56}B_2N_2$	$C_{68}H_{72}B_2N_2$
Formula weight [g mol^{-1}]	714.48	826.68	938.89
Temperature [K]	200(2)	100(2)	100(2)
Wavelength [Å]	0.71073	1.54178	0.71073
Crystal system	Monoclinic	Monoclinic	Triclinic
Space group	*C*2/c	*P*2$_1$/c	*P*-1
a [Å]	26.1224(8)	27.7304(12)	9.5981(5)
b [Å]	8.3077(3)	9.0103(4)	11.9160(5)
c [Å]	18.9832(6)	18.6100(8)	25.0597(11)
α [°]	90	90	85.521(2)
β [°]	106.476(2)	98.171(2	89.469(2)
γ [°]	90	90	89.876(2)
Volume [Å^3]	3950.5(2)	4602.7(3)	2857.2(2)
Z	4	4	2
Density (calculated) [Mg m^{-3}]	1.201	1.193	1.091
Absorption coefficient [mm^{-1}]	0.068	0.509	0.062
F(000)	1504	1760	1008
Crystal size [mm^3]	0.42×0.26×0.09	0.20×0.17×0.06	0.15×0.14×0.12
Theta range for data collection [°]	2.72 to 25.05	1.609 to 66.688	0.815 to 26.432
Index ranges	-30<=h<=30 -8<=k<=9 -22<=l<=21	-33<=h<=33 -10<=k<=7 -22<=l<=22	-12<=h<=6 -14<=k<=14 -30<=l<=31
Reflections collected	12578	36127	46207
Independent reflections	3422 [R(int) = 0.0340]	8142 [R(int) = 0.0269]	11612 [R(int) = 0.0474]
Absorption correction	multi-scan	Semi-empirical from equivalents	Semi-empirical from equivalents
Max. and min. transmission	0.9939 and 0.9718	0.9492 and 0.7249	0.9485 and 0.8865
Refinement method	Full-matrix least-squares on F^2	Full-matrix least-squares on F^2	Full-matrix least-squares on F^2
Data / restraints / parameters	3422 / 0 / 253	8142 / 0 / 585	11612 / 264 / 745
Goodness-of-fit on F^2	1.018	1.026	1.046
Final R indices [I>2sigma(I)]	R_1 = 0.0558 wR_2 = 0.1639	R_1 = 0.0381 wR_2 = 0.0961	R_1 = 0.0680 wR_2 = 0.1751
R indices (all data)	R_1 = 0.0782 wR_2 = 0.1786	R_1 = 0.0404 wR_2 = 0.0981	R_1 = 0.1124 wR_2 = 0.1989
Largest diff. peak and hole	0.258 and -0.453 e.Å^{-3}	0.245 and -0.255 e.Å^{-3}	0.295 and -0.282 e.Å^{-3}

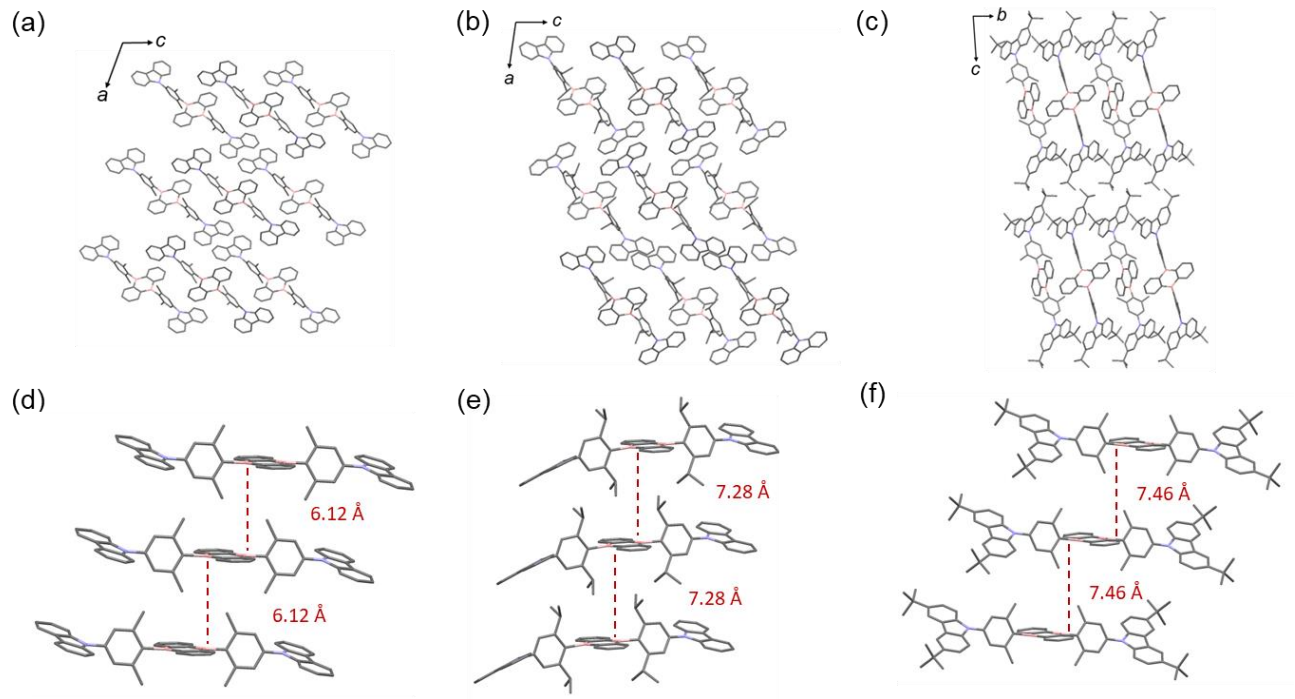

Fig. S8 The crystal packing of (a) CzDBA, (b) iCzDBA, and (c) *t*BuCzDBA. And the closest distances in single-crystal cell of (d) CzDBA, (e) iCzDBA, and (f) *t*BuCzDBA. All hydrogen atoms in three structures have been omitted for clarity.

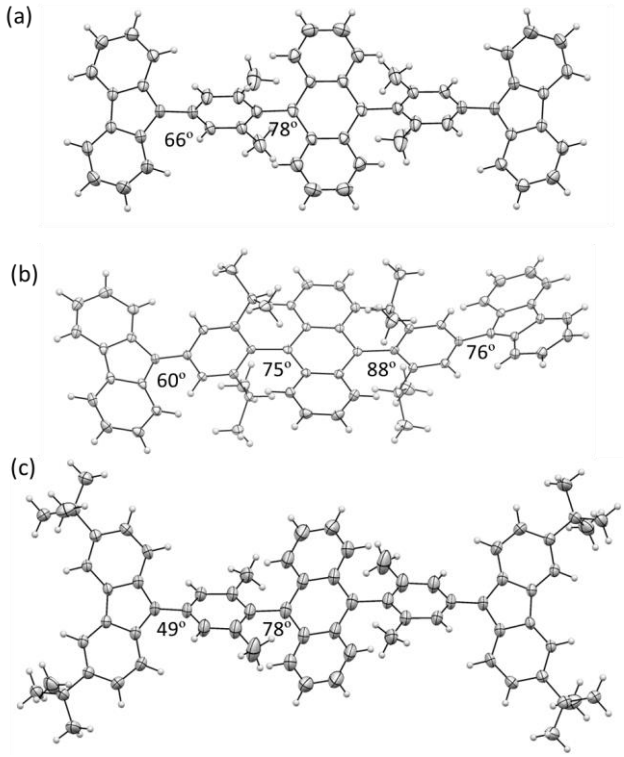

Fig. S9 The x-ray single-crystal structures and their dihedral angles for (a) CzDBA, (b) iCzDBA, and (c) *t*BuCzDBA.

(D) DFT methods and molecular dynamics

Table S2 Comparison of experimental and calculated singlet (S_1), triplet (T_1), and ΔE_{ST}

Methods	S_1 [eV]	T_1 [eV]	ΔE_{ST} [eV]	S_1 [eV]	T_1 [eV]	ΔE_{ST} [eV]	S_1 [eV]	T_1 [eV]	ΔE_{ST} [eV]
	*t*BuCzDBA			CzDBA			iCzDBA		
Experiment	2.486	2.464	0.022	2.629	2.596	0.033	2.607	2.574	0.033
B3LYP	1.894	1.887	0.007	2.034	2.023	0.011	2.100	2.091	0.009
CAM-B3LYP	3.112	2.683	0.428	3.189	2.681	0.508	3.275	2.728	0.547
PBE0	2.088	2.076	0.012	2.225	2.207	0.018	2.298	2.283	0.016
BMK	2.551	2.517	0.034	2.655	2.616	0.039	2.729	2.685	0.044
M06-2X	3.017	2.763	0.254	3.097	2.759	0.337	3.186	2.836	0.350
ωB97X-D	3.364	2.783	0.581	3.425	2.780	0.645	3.485	2.839	0.645

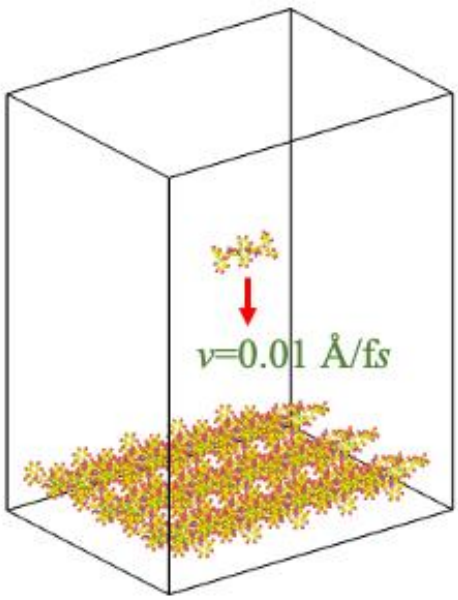

Fig. S10 The model setup for nonequilibrium molecular dynamics, periodic boundary conditions were applied along *x*, *y* and *z* directions. DBA molecule was subject to an initial velocity v=0.01 Å/f*s* from the top of simulation box and deposited to the subtract for every 5 p*s*.

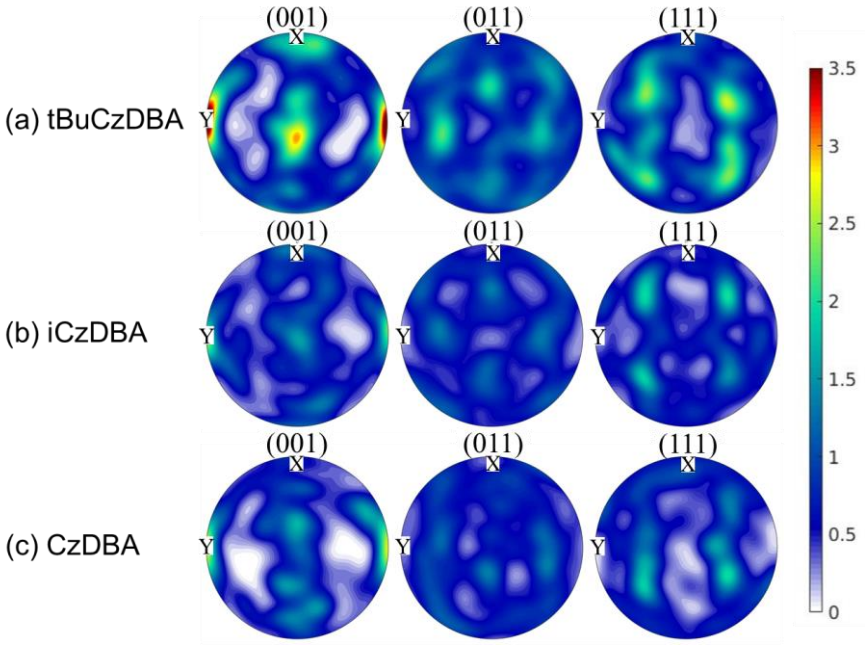

Fig. S11 The orientation of amorphous layer using stereographic projections. Panel (a) shows the pole figure of *t*BuCzDBA layer in (001), (011), and (111) direction. (b) shows the pole figure of iCzDBA layer in (001), (011), and (111) direction and (c) shows the pole figure of CzDBA layer in (001), (011) and (111) direction.

Table S3 Parameters of nonequilibrium molecular dynamics

Compound	CzDBA	iCzDBA	BuCzDBA
Box size[Å^3]	85×113×144	93×96×160	98×83×138
Forcefield	Dreiding	Dreiding	Dreiding
Boundary	Periodic	Periodic	Periodic
Deposition temperature	600K	600K	600K
Deposition velocity	5 ps per molecule 0.01 Å/fs	5 ps per molecule 0.01 Å/fs	5 ps per molecule 0.01 Å/fs
Cooling temperature	NVT 300K	NVT 300K	NVT 300K
Cooling time [ps]	1000	1000	1000
Time step [fs]	1	1	1
Number of deposited molecules after cooling	48	53	57

(E) Photophysical properties

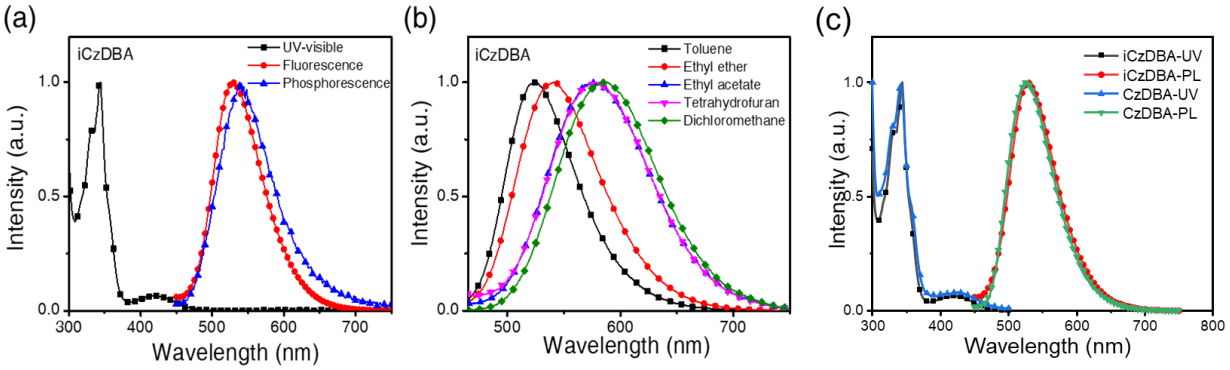

Fig. S12 (a) The UV-Vis absorption (black line) and fluorescence spectra (red line, Fl) of iCzDBA measured at 300 K in toluene (10^{-5} M) and CBP film (10 wt%). The phosphorescence (blue line, Ph) spectrum measured at 77 K in CBP film (10 wt%). (b) The PL spectra of iCzDBA at 300 K measured in various solvents. (c) The UV-Vis absorption spectra of iCzDBA (black line) and CzDBA (blue line); PL spectra of iCzDBA (red line) and CzDBA (green line) measured at 300 K in CBP film (10 wt%).

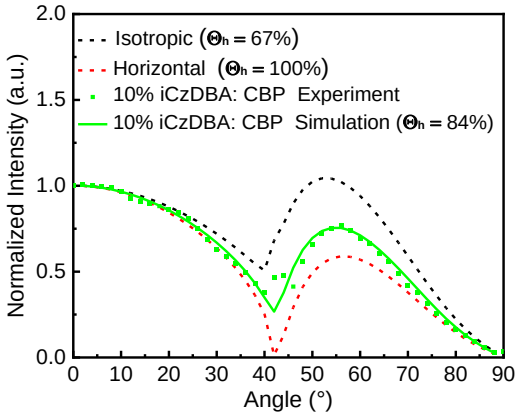

Fig. S13 The variable-angle PL measurement of 10 wt% iCzDBA in CBP films.

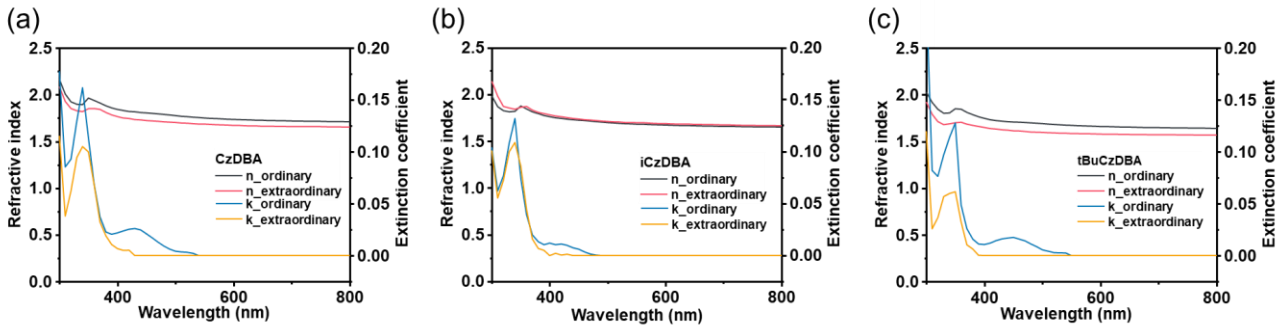

Fig. S14 Refractive indices (n) and extinction coefficient (k) of (a) CzDBA, (b) iCzDBA, and (c) *t*BuCzDBA.

Table S4 Photophysical properties of all DBA emitters

	Doped film[a)]						Neat film[b)]		
Emitter	Abs [nm][a)]	Fl [nm][a)]	Ph [nm][a)]	ΔE_{ST} [meV][a)]	PLQY [%][a)]	Θ_h [%][a)]	Fl [nm][b)]	PLQY [%][b)]	Θ_h [%][b)]
CzDBA	342	524	520	33	100	84	540	90.6	88
iCzDBA	344	528	538	33	95.2	84	538	88.0	77
*t*BuCzDBA	348	553	557	22	86.0	83	561	84.0	92

Photophysical properties of [a)]doped (10% DBAs: 90% CBP) film and [b)]DBAs neat film: Absorption (Abs), fluorescence (Fl) maximum at 300 K and phosphorescene (Ph) maximum at 77 K in 30-nm-thick films, the energy gap (ΔE_{ST}) was defference between S_1 and $T_{1,}$. Absolute total PLQY of 50 nm-thick films using an integrating sphere. Θ_h was meareasured and fitted by using the variable-angle PL measurement of 30 nm-thick films.

Table S5 Transient PL results and rate constants of DBA compounds

	τ_p [ns][c)]	τ_d [μs][c)]	Φ_p [%][d)]	Φ_d [%][d)]	k_p [10^7 s^{-1}][e)]	k_d [10^6 s^{-1}][f)]	k_r [10^6 s^{-1}][g)]	k_{IC} [10^6 s^{-1}][h)]	k_{ISC} [10^7 s^{-1}][i)]	k_{RISC} [10^6 s^{-1}][j)]
CzDBA[a)]	34	1.0	38.4	52.2	2.94	1.00	11.3	1.17	1.69	2.36
*t*BuCzDBA[a)]	36	1.2	34.7	49.3	2.78	0.83	9.64	1.84	1.63	2.02
iCzDBA[a)]	65	1.4	32.7	55.3	1.54	0.71	5.03	0.69	0.97	1.92
iCzDBA[b)]	29	2.9	17.0	78.2	3.45	0.34	5.86	0.30	2.83	1.93

[a)] DBA compounds measured in neat films at 300 K. [b)] 10 wt% iCzDBA measured in CBP film (30 nm) at 300 K. [c)] The prompt lifetime (τ_p) component and the delayed lifetime (τ_d). [d)] The prompt fluorescent (Φ_p) component and the delayed fluorescent (Φ_d) component of PLQY. [e)] The rate constant of prompt component (k_p). [f)] The rate constant of delayed component (k_d). [g)] The rate constant of radiative decay (k_r). [h)] The rate constant of internal conversion (k_{IC}). [i)] The rate constant of intersystem crossing (k_{ISC}). [j)] The rate constant of reverse intersystem crossing (k_{RISC}).

The rate constants of DBA compounds were determined by using reported methods as the following equations:

$$k_p = 1/\tau_p \quad \text{(S1)}$$

$$k_d = 1/\tau_d \quad \text{(S2)}$$

$$k_r = \Phi_p/\tau_p \quad \text{(S3)}$$

$$\Phi_p + \Phi_d = k_r/(k_r + k_{\mathrm{IC}}) \quad \text{(S4)}$$

$$\Phi_p = k_r/(k_r + k_{\mathrm{IC}} + k_{\mathrm{ISC}}) \quad \text{(S5)}$$

$$\Phi_{\mathrm{ISC}} = k_{ISC}/(k_r + k_{\mathrm{IC}} + k_{\mathrm{ISC}}) \quad \text{(S6)}$$

$$\Phi_{\mathrm{RISC}} = \Phi_d/\Phi_{\mathrm{ISC}} \quad \text{(S7)}$$

$$k_{\mathrm{RISC}} = \frac{k_p k_d \Phi_d}{k_{\mathrm{ISC}} \Phi_p} \quad \text{(S8)}$$

(F) Characteristics of nondoped and ultrathin EML devices

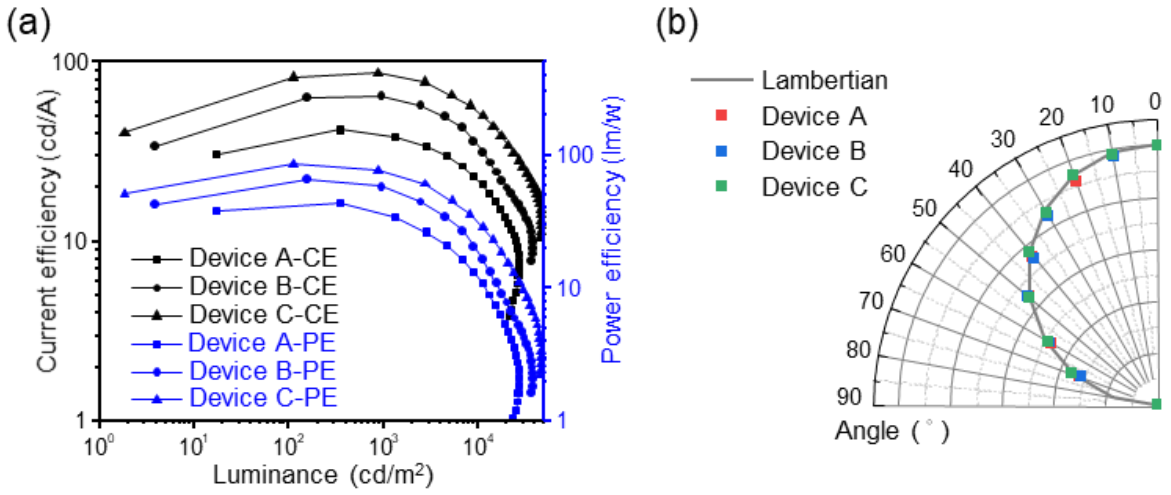

Fig. S15 (a) Current efficiency (CE) and power efficiency (PE) versus luminance plot of device A, B, and C. (b) Angular dependence of EL intensities with the Lambertian distributions of device A, B and C. The emission distributions of three devices are nearly Lambertian pattern.

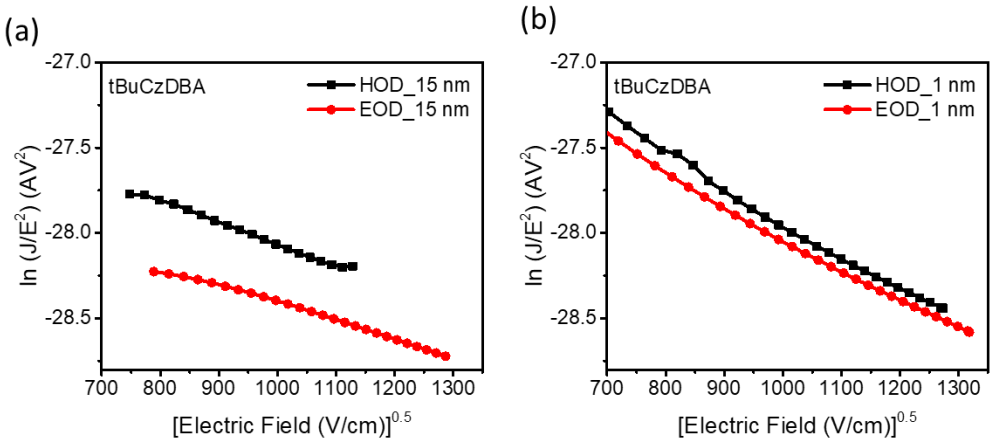

Fig. S16 The hole-only device (HOD) and electron-only device (EOD) of (a) 15 nm *t*BuCzDBA and (b) 1 nm *t*BuCzDBA.

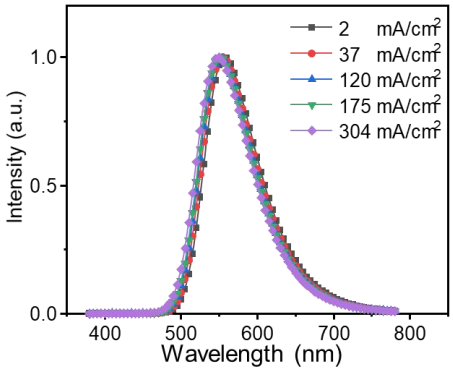

Fig. S17 The EL spectra of device U3 at various current densities.

Table S6 Charge mobilities of *t*BuCzDBA

Thickness	1 nm		15 nm	
Mobility	μ_e (cm^2/Vs)	μ_h (cm^2/Vs)	μ_e (cm^2/Vs)	μ_h (cm^2/Vs)
tBuCzDBA	$1.64*10^{-6}$	$1.78*10^{-6}$	$6.48*10^{-6}$	$1.13*10^{-5}$

Table S7 Summary of recent nondoped TADF OLEDs with EQE near or over 20%

Material	λ_{EL} (nm)	V_{on} (V)	η_{EQE} (%)	CE (cd/A)	PE (lm/W)	Thickness (nm)	Reference
*t*BuCzDBA	558	2.4	26.9	86.9	86.3	15	This work
*t*BuCzDBA	553	2.2	24.5	82.9	95.3	5	This work
*t*BuCzDBA	552	2.1	22.0	70.2	88.2	1	This work
DMAC-DPS	480	4.3	19.5	-	19	30	*Adv. Mater.* **2015**, *27*, 2096
DMAC-BP	510	2.6	18.9	-	59	30	*Adv. Mater.* **2015**, *27*, 2096
DMAC-TRZ	500	3	20	61.1	45.7	20	*Chem. Commun.* **2015**, *51*, 13662
B-oTC	474	3.9	19.1	37.3	27.6	40	*Angew. Chem. Int. Ed.* **2017**, *56*, 15006
MPAc-BS	487	3.4	22.8	49.9	41.4	30	*Adv. Funct. Mater.* **2018**, *28*, 1802031
DCB-BP-PXZ	548	2.5	22.6	72.9	81.8	35	*Angew. Chem. Int. Ed.* **2018**, *57*, 9290
CzDBA	560	2.1	19	-	87	80	*Nat. Photon.* **2019**, *13*, 765
2Cz-DPS	518	4.1	28.7	82.3	51.8	30	*Chem. Sci.* **2019**, *10*, 8129
2tCz2CzBn	470	2.7	21.6	31.1	-	30	*Adv. Sci.* **2020**, *7*, 1902508
TP2P-PXZ	548	2.6	25.4	84.1	96.5	20	*Angew. Chem. Int. Ed.* **2021**, *60*, 25878
CzPh2AQ	575	~5.5	22.1	54.4	28.5	28	*Chem. Eng. J.* **2022**, *442*, 136219
3CPDA-MPC	525	4.6	26.5	65.0	42.1	30	*Adv. Funct. Mater.* **2022**, 2112881
9CPDA-MPC	510	3.6	29.6	84.1	64.4	30	*Adv. Funct. Mater.* **2022**, 2112881